Dynamic Calibration of Multiple Data Types

Thomas Kelecy, Emily Lambert and Benjamin Sunderland
L3Harris – Applied Defense Solutions
Vivek Desai
University of Texas, Austin

ABSTRACT

The research presented here builds on previous research which investigated the dynamic calibration of electro-optical sensor data used to support space situational awareness. The research expands the dynamic calibration approach to include radar sensor data, examines techniques for consolidating optical and radar measurements, and establishes methods for determining sensor quality information including long term trends and biases.

Calibrating and establishing trust in new or third-party sensors within the space situational awareness architecture is a difficult and lengthy process, often taking a number of years. Techniques that would enable more rapid assessment of third-party sensors and determination of their data quality and integrity would enable external sensors to be utilized more readily and significantly improve the space operational awareness.

The proposed research activity would draw on radar data from commercial network providers and other publicly available range observation sources. The results of the research would be equally applicable however to sensors operating in the classified domain. The dynamic Unscented Schmidt Kalman Filter (USKF) algorithms, already established for optical sensor calibration, is tested and validated for multiple data and multi-sensor calibration with emphasis on range data calibration.

1. BACKGROUND AND MOTIVATION

There is a growing need to supplement the existing space surveillance sensor networks with additional sensors to support tracking and management of the ever-increasing population of both active and inactive Earth orbiting Resident Space Objects (RSOs) in all orbit regimes [1]. The Geosynchronous Earth Orbit (GEO) regime, in particular, is a "limited resource" given the special operational geometry it affords commercial and military users [2, 3, 4]. A globally distributed network of "trusted sensors" including both electro-optical (EO) sensors and range-providing sensors – e.g. radar, laser ranging, and Global Positioning System (GPS) pseudo-range – ensures timely and actionable monitoring of the space domain to help maximize safe use of space for communications, commerce, defense, and Earth science missions. There is a need for rapid validation and near real-time (NRT) data integrity monitoring to facilitate rapid, confident, and appropriately weighted incorporation of new or upgraded sensors into a network. Not all sensors tracking RSOs in the GEO regime have ready access to reference satellites (i.e. fiducials) needed for sensor calibration, hence, this work proposes an approach to enable a robust and dynamic globally accessible means for sensor data validation that includes establishing a set of "trusted" RSO's in multiple orbit regimes.

This paper is an extension of work [5, 6] which proposed a dynamic filter as a key component of a data integrity assessment process to support improved orbital safety and EO sensor calibration. The results included in this paper extend the use of a multi-state filter to estimate combined RSO states and sensor specific biases utilizing both EO and range observations of multiple satellites. A baseline set of sensor data, which includes at least one of the sensors tracking a known reference satellite, was analyzed to establish a "trusted" sensor network and reference RSO's for validation of the automated NRT sensor calibration and quality assessment. A dynamic Kalman-like filter implementation was developed which uses the NRT estimation of sensor noise and bias characteristics and includes facilitation of an NRT reference satellite orbit state to enable sensor calibration. The performance results are demonstrated with measurement data from two EO sensors and two range sensors to demonstrate improvements to results when multiple sensor data sources are generating positive detections. The fusion of multiple data types and sources will also maximize the distinction between filter "artifacts" (e.g. apparent but not actual trajectory structure) due to data quality and anomalies versus unmodeled dynamics of the tracked objects in the estimation filter [7].

The concept of operations (CONOPS) that supports this is illustrated in Fig. 1 where the stages of the process transition through the following stages: (1) no trusted sensors or reference satellites are available, (2) a reference satellite is identified and an un-validated sensor is tasked to track it, (3) a sensor is calibrated and is used to establish additional trusted RSO's, (4) the full network of trusted sensors is established using the trusted RSO's derived from the orbit estimation process. The criteria for a sensor being trusted is established when a stable set of biases and noise levels are reached. These are derived from the pre- and post-fit residuals and other tests such as the "filter-smoother consistency test" [8]. Similarly, a "trusted" RSO is established once its estimated state converges to an acceptable threshold and the consistencies are stable [9].

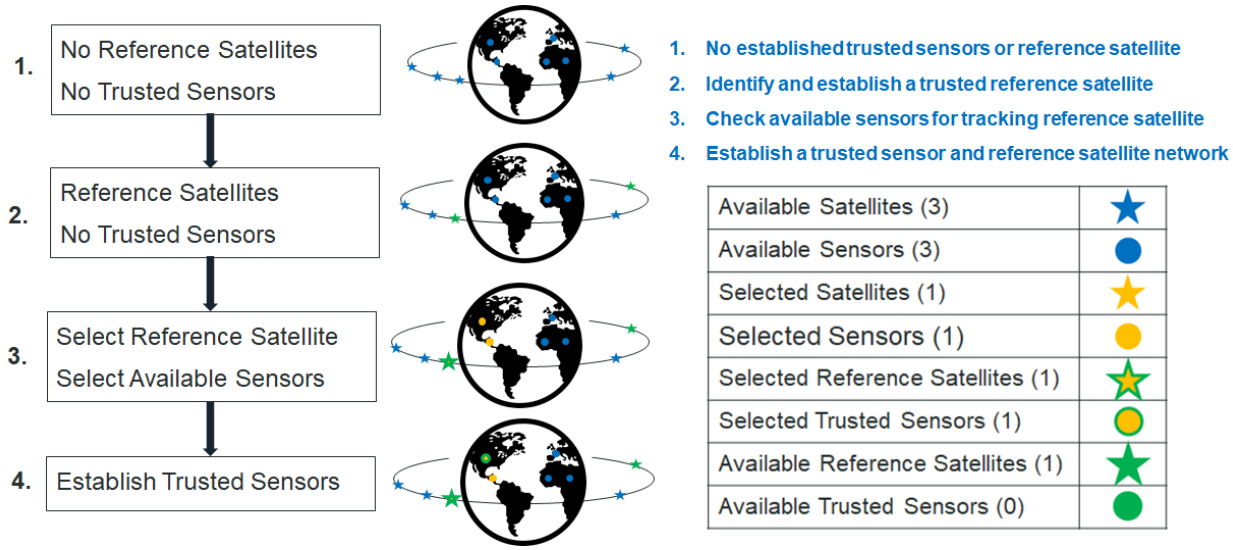

Fig. 1. Stage of establishing a trusted network

In the second section of this paper, the "multi-state dynamic filter" is formulated using the Unscented Schmidt Kalman Filter (USKF) and its implementation for the NRT dynamic calibration of EO and range data is described. Analysis results for a representative 8-satellite, 4-sensor (2-EO and 2-range) use-case is presented to demonstrate the utility of the technique. Conclusions are summarized and future work includes development and operational implementation of the dynamic USKF for sensor networks for managing multiple sensor data types.

2. DYNAMIC CALIBRATION FORMULATION AND IMPLEMENTATION

There are a number of specific analytical tools that can be exploited as a part of the measurement data integrity process, most of which implement the same models and algorithms that are used in orbit determination (OD) and prediction processing. These techniques, which can be exercised in conjunction with the OD process, have been summarized in previous work [5, 9]. The DARPA Orbit Outlook (O2) project [10] was established with the purpose of exploring how to integrate non-traditional sensor data from different sources. We extend O2 capabilities in this work to include the addition of range which is now being provided by commercial providers [11].

The OD and prediction process is a foundational capability of data integrity processing. It assumes (a) *a priori* knowledge of the measurement noise statistics, (b) any measurement biases have been accounted for, and (c) the appropriate fidelity of the dynamic models is being used for the estimation and prediction. In reality, any combination of these assumptions can be invalid; establishing a causal relationship for unexpected behavior in the sensor data processing can be challenging due to ambiguities in the possible information and modeling sources and how they manifest themselves in the performance metrics. In other words, actual RSO motion is governed by the physics of astrodynamics. However, perceived RSO motion has contributions from astrodynamics as well as information sources and modeling assumptions including model limitations. The "consider covariance" implementation, described in the next section, addresses a method for accommodating modeling errors or so-called "known unknowns". To address this, some additional tools have been proposed that apply state-of-the-art

information theory. "Consider covariance" has been a long-established method for assessing the effects of unmodeled observation and dynamic errors on the estimation and prediction performance [12].

A "global", multi-state filter approach is presented in the next section which includes all RSO and sensor parameters in a single estimation filter. This implementation enables information to be "shared" between state elements via the correlation matrix, thus enhancing the ability to manage data quality from multiple sensors and assess data anomalies. This approach supports the growing trend towards using "persistent monitoring" through a network of EO sensor arrays which "stare" along the GEO belt to monitor RSO activity. Though these networks can provide nearly continuous monitoring, the downside may be that one or more of the fixed sensors may not have immediate access to a designated reference satellite. Such sensors will benefit from other sensors in the network that do have access to reference satellites and leverage this information via the multi-state filter.

Unscented Schmidt Kalman Filter Implementation

The proposed dynamic calibration, to be exercised in NRT, requires an estimation implementation that enables certain parameters to be estimated while others are only considered during the estimation process, e.g. measurement biases, until the appropriate reference satellite data are available. This section outlines the formulation.
In order to account for, or "consider", the uncertainty associated with non-estimated parameters, the unscented Schmidt-Kalman filter (USKF) is utilized. It incorporates the "consider covariance analysis" concept whereby known errors in model and state parameters can be "considered" to make the estimation uncertainty more representative (realistic). This enables a user to account for so-called *"*known unknowns". Using by-products of the USKF algorithm, the Fisher information [5] can be computed, giving a measure of the observability of estimated and considered parameters.

Stauch and Jah [13] presented the USKF which is well suited for this application. There are two general categories of consider techniques. One is consider analysis, in which a typical state filter is executed and, after the measurement update, the uncertainties of the consider parameters are mapped into the state space. The other technique is a consider filter, in which the state itself is augmented with the consider parameters while the consider parameters' values and uncertainties are forced to be unchanged. Thus, the consider parameters are directly included in the filtering process. The USKF algorithm used in this work is given in Table 1.

Note that $Z_{i,k}$ and $P_{zz,k}$ are the augmented state and covariance (i.e. both estimated and considered parameters). Notice that the key difference between the USKF and the standard Unscented Kalman Filter (UKF) is that the update to the consider state and covariance terms are forced to be zero, while the consider-estimated parameter cross-covariance term updates are maintained. This makes the USKF a sub-optimal filter but one that is useful in preventing a falsely optimistic estimate. This is sometimes referred to as "covariance realism." Parameters such as measurement related biases can be considered until reference satellite data are available to support calibration of the sensor.

Parameters in an estimator can either be ignored, considered or estimated (referred to as "ICE"). In this application, the state consists of satellite position, velocity, CrA/m (Coefficient of reflectivity times area divided by mass (i.e. the effect of solar radiation pressure (SRP)), and sensor related biases (e.g. *Time-tag bias*). In some instances, some of these filter parameters may not be "observable," i.e., there is insufficient information in the observations to estimate them. In this case, we might "consider" the parameter – that is, account for our knowledge of its uncertainty in the filter estimates and covariance without estimating it.

This work examines the improvements to filter convergence when a reference satellite state is available. If a reference state is available, the process initializes the filter by including the reference orbit information in the state at a point in time just prior to the first EO data time-tag. At the point where EO data and the reference information are both available, the sensor bias can then be estimated until that parameter is sufficiently converged. At that point, the EO data should be monitored for consistency over a specified time span before it can be completely trusted. In other words, does the hypothesized bias achieve some steady state in the presence of increasing evidence? A "data lake" consisting of both "raw" as well as calibrated data can be accessed and, when a reference is available, a sensor bias can be directly estimated. If no reference satellite is available for an EO sensor, then its quality can be indirectly assessed in the multi-state filter implementation and the resulting performance metrics can then be included in the data repository for other users to access and/or contribute to. This process, illustrated in Fig. 2, provides performance metrics which can be applied to distinguish between data artifacts and dynamic phenomena [7, 9].

Note there are “synchronous” and “asynchronous” functions. The process elements shown in blue are the USKF and “trust” metric validation processes whereas the data pre-conditioning and management are depicted in yellow and assume the data have been pre-correlated to known RSO tracks. The overall process establishes a validation and data integrity infrastructure consisting of trusted sensors and reference RSO’s that can be used to validate new sensors or establish new reference RSO’s.

Table 1. USKF Formulation

USKF
Predictive
$\mathbf{S}_{zz,k-1} = Cholesky(\mathbf{P}_{\boldsymbol{zz},k-1})$
$\boldsymbol{Z}_{i,k-1} = \hat{\boldsymbol{z}}_{k-1} \pm \sqrt{n_x + n_c}\boldsymbol{s}_{i,k-1}$
where $\mathbf{S}_{zz} = [\boldsymbol{s}_1, ..., \boldsymbol{s}_{n_x+n_c}]$
$w = \frac{1}{2(n_x+n_c)}$
$\boldsymbol{Z}_{i,k} \Leftarrow \dot{\boldsymbol{Z}}_i = \boldsymbol{f}(\boldsymbol{Z}_{i,k-1}, t)$
$\hat{\boldsymbol{z}}_k = \sum_{i=1}^{2(n_x+n_c)} w_i \boldsymbol{Z}_{i,k}$
$\mathbf{P}_{\boldsymbol{zz},k} = \sum_{i=1}^{2(n_x+n_c)} w_i(\boldsymbol{Z}_{i,k} - \hat{\boldsymbol{z}}_k)(\boldsymbol{Z}_{i,k} - \hat{\boldsymbol{z}}_k)^T$
Corrective
$\boldsymbol{Y}_i = \boldsymbol{h}(\boldsymbol{Z}_i, t)$
$\hat{\boldsymbol{y}} = \sum_{i=1}^{2(n_x+n_c)} w_i \boldsymbol{Y}_i$
$\mathbf{P}_{\boldsymbol{yy}} = \sum_{i=1}^{2(n_x+n_c)} w_i(\boldsymbol{Y}_i - \hat{\boldsymbol{y}})(\boldsymbol{Y}_i - \hat{\boldsymbol{y}})^T + \boldsymbol{R}$
$\mathbf{P}_{\boldsymbol{zy}} = \sum_{i=1}^{2(n_x+n_c)} w_i(\boldsymbol{Z}_i - \hat{\boldsymbol{z}})(\boldsymbol{Y}_i - \hat{\boldsymbol{y}})^T$
$\begin{bmatrix} \mathbf{P}_{\boldsymbol{xy}} \\ \mathbf{P}_{\boldsymbol{cy}} \end{bmatrix} = \mathbf{P}_{\boldsymbol{zy}}$
$\mathbf{K}_z = \mathbf{P}_{\boldsymbol{zy}}\mathbf{P}_{\boldsymbol{yy}}^{-1} = \begin{bmatrix} \mathbf{K}_{\boldsymbol{x}} \\ \mathbf{K}_{\boldsymbol{c}} \end{bmatrix} \begin{pmatrix} NOTE: \\ \mathbf{K}_{\boldsymbol{c}} \neq 0!! \end{pmatrix}$
Force correction to consider terms to be 0:
$\hat{\boldsymbol{z}}^+ = \hat{\boldsymbol{z}}^- + \begin{bmatrix} \mathbf{K}_{\boldsymbol{x}} \\ \mathbf{0} \end{bmatrix} (\boldsymbol{y} - \hat{\boldsymbol{y}})$
$\mathbf{P}_{\boldsymbol{zz}}^+ = \begin{bmatrix} \mathbf{P}_{\boldsymbol{xx}}^- & \mathbf{P}_{\boldsymbol{xc}}^- \\ \mathbf{P}_{\boldsymbol{cx}}^- & \mathbf{P}_{\boldsymbol{cc}}^- \end{bmatrix} - \begin{bmatrix} \mathbf{K}_{\boldsymbol{x}}\mathbf{P}_{\boldsymbol{yy}}\mathbf{K}_{\boldsymbol{x}}^T & \mathbf{K}_{\boldsymbol{x}}\mathbf{P}_{\boldsymbol{yy}}\mathbf{K}_{\boldsymbol{c}}^T \\ \mathbf{K}_{\boldsymbol{c}}\mathbf{P}_{\boldsymbol{yy}}\mathbf{K}_{\boldsymbol{x}}^T & \mathbf{0} \end{bmatrix}$

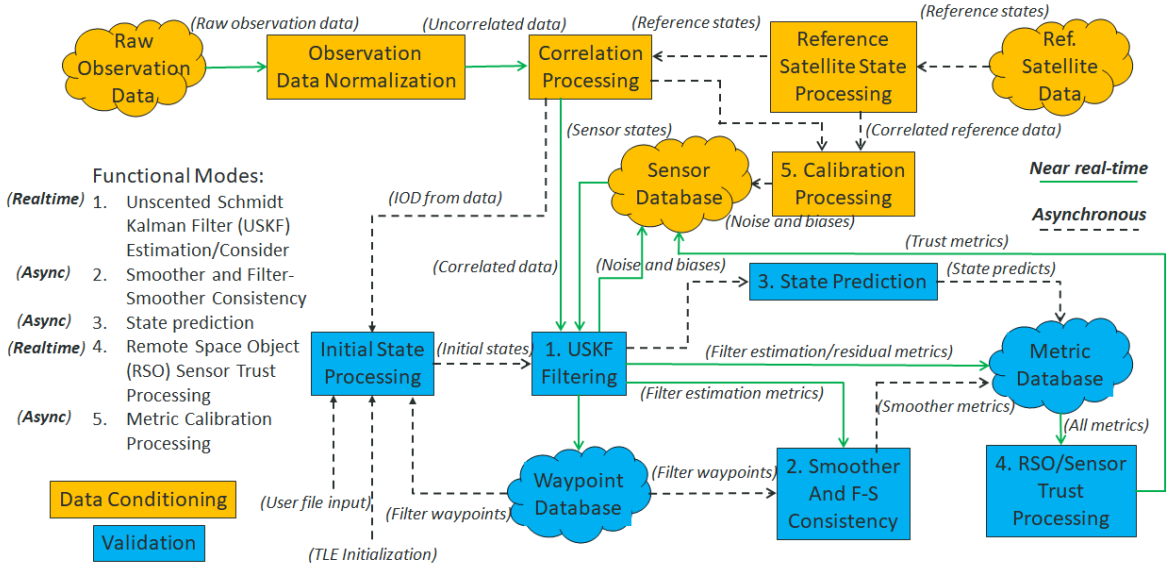

Fig 2. Estimation and Consider Process

USKF Timing and Range Bias Formulation

The subsequent use-cases model a sensor timing or range bias to illustrate the near real-time calibration using the USKF. To accommodate the ability to either estimate or consider the timing or range biases, they must be included in the USKF state along with any other estimated parameters (e.g. *position, velocity and CrA/m*). The biases are observable in the USKF via the EO and range reference measurements derived from a reference satellite (RSO). The reference satellite is tracked by the EO and range sensors and, given the sensor inertial states (derived from the site coordinates) at the measurement time, affords a reference measurement to which the actual measurements are compared. Any resulting bias is manifested in the residuals. At the time of each measurement update, the state-vector sigma points are used to compute an equivalent measurement sigma points and these are adjusted for the current best estimate of the timing bias as follows

$$t_{corrected} = t_{observation} - t_{bias} \tag{1}$$

where the reference line-of-site vector is derived from

$$\vec{R}_{J2000} = \left[T_{ITRF \to J2000}(t_{corrected})\right] \vec{R}_{ITRF} \tag{2}$$

$$\vec{\rho} = \vec{r}_{J2000} - \vec{R}_{J2000} - \vec{v}_{J2000} \cdot (t_{bias} + \delta t_{LTC}) \tag{3}$$

and the range, right ascension and declination reference measurement sigma-points are computed as the following

$$\rho = \|\vec{\rho}\| = \sqrt{\rho_x^2 + \rho_y^2 + \rho_z^2} \tag{4}$$

$$\alpha = \tan^{-1}\left(\frac{\rho_y}{\rho_x}\right) \tag{5}$$

$$\delta = \sin^{-1}\left(\frac{\rho_z}{\rho}\right) \tag{6}$$

These are subsequently used in the USKF measurement update step of the filter process.

Multi-state Tracking Concept

The idea behind the multi-satellite, multi-sensor scenario is presented conceptually in Fig. 3; this illustrates how the filter would leverage common observations to provide information needed to estimate biases and assess performance for a 2-satellite, 2-EO sensor scenario. An outline of the process to be implemented is as follows:

1. Collect EO data (Optical 1) on a designated Reference Satellite (RefSat).
2. Acquire the reference satellite data and derive reference measurements.
3. Refine the orbit of the tracked RefSat (e.g. SRP estimation) using the reference data.
4. Estimate sensor noise and biases for the EO sensor (Optical 1) using the EO data and the refined reference satellite state.
5. Use the EO site with updated biases (Optical 1) to track a satellite in common (RSO) with another optical site (Optical 2).
6. Use RSO data as a “reference" for calibrating the second EO sensor (Optical 2).
7. Continue to develop a network of “trusted” sensors using a multi-state filter which incorporates assessment of data and states to determine data integrity of newly included EO and range sensors and monitor existing sensors.

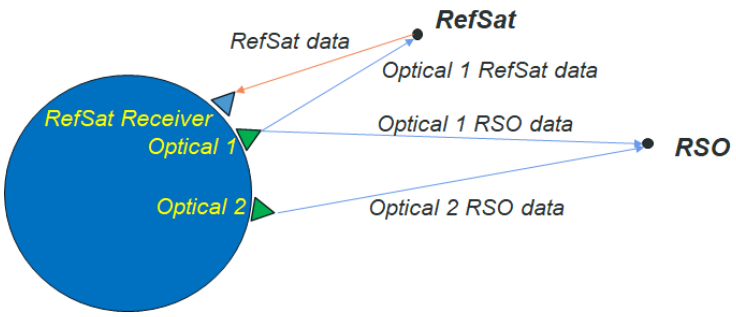

Fig. 3. 2-satellite / 2-sensor Use Case Scenario Two-Satellites and Two-Sensors Simulation Results

An 8-satellite, 2-EO sensor and 2-range sensor scenario was simulated which included both reference data and EO tracking of a GPS reference satellite (GPS-NAV-72) and those details are presented in the next section. To illustrate the USKF application to a multi-state filter, a 2-satellite state filter is described here, one for the reference, X_{ref}, and one for the GEO RSO, X_{rso},

$$\vec{X} = \begin{bmatrix} \vec{X}_{ref} \\ \vec{X}_{rso} \\ \delta\vec{t} \\ \delta\vec{\rho} \end{bmatrix} \tag{7}$$

where the reference state is

$$\vec{X}_{ref} = \begin{bmatrix} \vec{r}_{ref} \\ \vec{v}_{ref} \\ \gamma_{ref} \end{bmatrix} \tag{8}$$

the RSO state is

$$\vec{X}_{rso} = \begin{bmatrix} \vec{r}_{rso} \\ \vec{v}_{rso} \\ \gamma_{rso} \end{bmatrix} \tag{9}$$

the optical sensor bias state is

$$\delta\vec{t} = \begin{bmatrix} \delta t_1 \\ \delta t_2 \end{bmatrix} \tag{10}$$

$$\delta\vec{\rho} = \begin{bmatrix} \delta\rho_1 \\ \delta\rho_2 \end{bmatrix} \tag{11}$$

The two optical sensor biases assumed to be timing (other biases can be included in the state and estimated as appropriate) are δt_1 and δt_2. Similarly, the range sensor bias estimates are denoted as $\delta\rho_1$and $\delta\rho_2$. These are expanded as sigma-points as per the USKF implementation and are derived from the position and velocity sigma-points. The position and velocity Cartesian vectors for the reference and RSO are

$$\vec{r} = \begin{bmatrix} r_x \\ r_y \\ r_z \end{bmatrix} \tag{12}$$

$$\vec{v} = \begin{bmatrix} v_x \\ v_y \\ v_z \end{bmatrix} \tag{13}$$

and the relevant solar radiation pressure term for each is defined as

$$\gamma = C_r \frac{A}{m} \tag{14}$$

where C_r is the SRP coefficient, A is the effective cross-sectional area and m is the mass. The filter can be generalized for any number of reference satellites, RSOs, and tracking sensors, though the USKF implementation remains as previously described.

3. MULTI-SENSOR BIAS CALIBRATION: SCENARIO, ANALYSIS AND RESULTS

Analysis Scenario Background

There are eight RSO's being modeled as being tracked by two EO sensors, one in Southern Spain and one in South Africa, and each of the EO sensors has a "range" sensor co-located with it. This could be a commercial radar, or as assumed in this analysis, a GPS receiver measuring pseudo-range to a GPS satellite when it is in view. One of the eight RSO's is a GPS satellite which is also tracked by each of the EO sensors. The tracking geometry for the 8-satellite, 2-EO sensor / 2-range sensor scenario is shown in Fig 4 and the EO observations include lighting constraints. The IGU (International GNSS Service Ultra-Rapid orbit product) reference state data were also simulated for the GPS reference satellite and are used to test their influence on filter estimation performance when they are included in the filter processing.

The EO filter state errors and sigma values are shown in Table 2 and were modelled to have a noise value of 0.5 arc-seconds, 1-σ, per right ascension and declination component, whereas each of the IGU state components for the GPS reference satellite were generated with a 1-σ noise of 5 cm. The range measurements, when available, were modelled with a noise of 10 meters. The measurements were generated at a 60-second sample interval and the GPS reference state measurements at a 15-minute interval, consistent with the IGU files. EO sensor timing biases of 250 milliseconds for each of the Spain and South Africa optical sensors were used, and range biases of 500 m and 1000 m, for GPS tracker 2 and 3, respectively, were modeled. The satellite filter initial state error and filter parameters are given in Table 3 with SRP errors of 10% for each satellite being assumed.

Table 2. Sensor Filter State Errors

Sensor	Type	Observ. Noise	Observ. Units	Initial Bias	Filter Sigmas	Bias Units
SOUTHERN-SPAIN	EO-timing	0.5	arc-sec	0.25	0.5	seconds
SOUTH-AFRICA	EO-timing	0.5	arc-sec	0.25	0.5	seconds
GPS-TRACKER-2	range	10	meters	500	1000	meters
GPS-TRACKER-3	range	10	meters	1000	2000	meters

Table 3. Satellite Filter Initial State Configuration

	RefSat Initial Error	RefSat Filter Sigma	RSO Initial Error	RSO Filter Sigma
Px (km)	0.003	1.5	10	5
Py (km)	0.003	1.5	50	5
Pz (km)	0.003	1.5	5	5
Vx (km/s)	0.00003	0.5	0.5	0.5
Vy (km/s)	0.00003	0.5	0.1	0.5
Vz (km/s)	0.00003	0.5	0.05	0.5
CrA/m (m^2/kg)	0.01	0.05	0.01	0.05

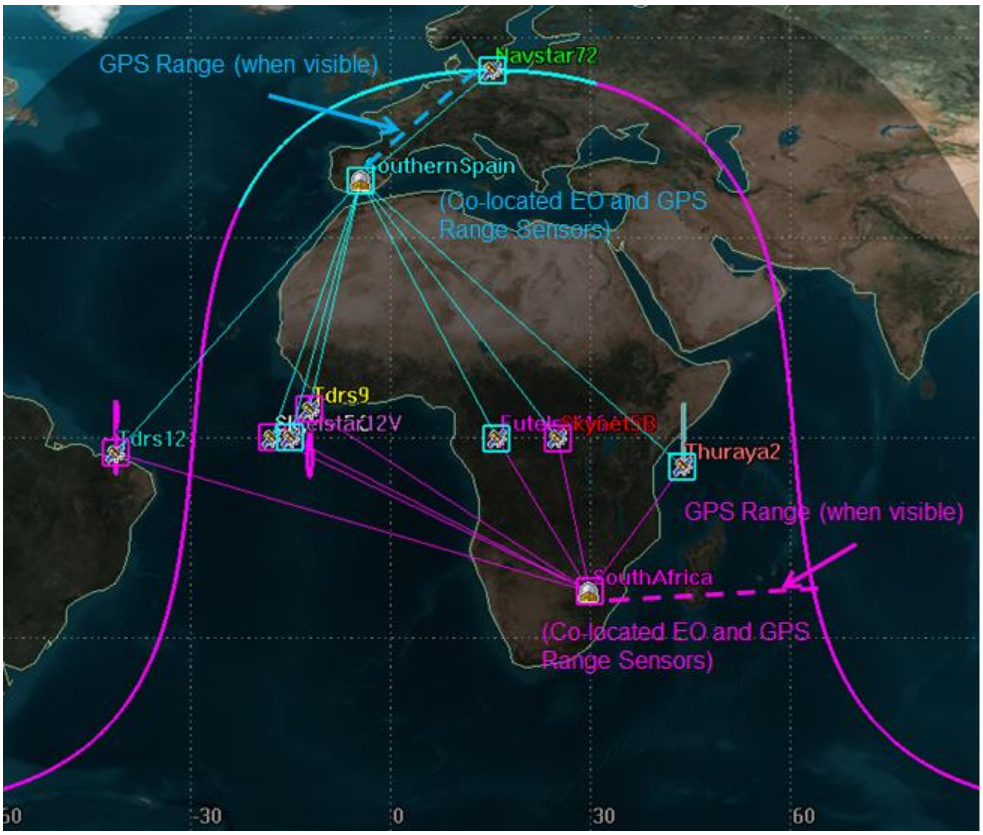

Fig. 4 Tracking Geometry for 8-satellite / 2-EO sensor / 2-range sensor use case

Analysis Results for when Reference Satellite is Included in the Filter

The analysis that was performed examined the filter performance when at least one of the EO sensors was able to track a GPS "reference satellite" for which an accurate reference state (ephemeris) is available. In this example the reference is GPS-NAV-72 and the IGU states, which is available in near real-time, are used as "pseudo-observations" to update the state in the filter. The simultaneous tracking by the EO sensor, Southern Spain in this case, enables the time bias for that sensor to be directly estimated. While the IGU states only include the Cartesian positions, use of them in the filter as observations also enables estimates of the velocity and SRP parameter to ensure accurate predictions in the multi-state filter to support accurate EO time bias calibration. Range biases for each of the GPS receivers were also modelled and estimated in the multi-state filter.

For the use case spanning 5+ hours (Fig. 4) the eight RSO satellite positions, velocities and SRP state parameters, in addition to the two EO sensor timing biases and the two GPS range biases were estimated for the two cases where (1) the GPS reference state was included and (2) the reference state was not included. The multi-state filter converged in both of these cases and the estimation error results (vs. the known "truth") for all estimated parameters are summarized for the RSO and sensor bias states in Tables 4 and 5, respectively.

As can be seen in Table 4, the RSO state estimates appear somewhat better for the case where a GPS reference state was included in the filter processing. It turns out that this is due to the filter taking longer to converge when no reference state is available; in most cases hours versus minutes when a reference state is available. Note also that the TDRS-12 and GPS-NAV-72 errors are larger in both cases than those of the other RSO's. Some insight can be gained by examining the results shown in Fig. 5 and 6 where Fig. 5 shows that the TDRS-12 state takes a bit longer to converge as compared to TDRS-9. This is likely due to the differences in geometry which is more obvious when examining Fig. 4 more closely. Fig. 6 shows that the GPS RSO state also takes a bit longer to converge so those error statistics are also reflected in the higher errors shown in Table 4.

Table 4. Filter RSO State Estimation Results for Reference State Sensitivity

		With Refernce State			Without Reference State		
Satellite	SSN	Pos RSS (m)	Vel RSS (m/s)	CrA/m (m^2/kg)	Pos RSS (m)	Vel RSS (m/s)	CrA/m (m^2/kg)
TDRS-9	27389	167.656	0.99459	0.0019	312.149	1.31214	0.0072
Thuraya-2	27825	176.773	1.12580	0.0025	235.111	1.01683	0.0031
Skynet-5B	32294	170.736	0.44420	0.0035	223.800	0.62715	0.0079
Skynet-5C	33055	176.878	0.83638	0.0062	281.385	1.17439	0.0040
Eutelsat-16A	37836	200.594	1.65618	0.0068	232.552	0.97134	0.0068
TDRS-12	39504	4342.460	17.63488	0.0008	4319.139	13.20361	0.0012
GPS-NAV-72	40294	2049.865	4.54156	0.0202	2594.493	5.93933	0.0060
Telstar-12V	41036	276.637	2.15945	0.0036	247.445	1.67632	0.0030

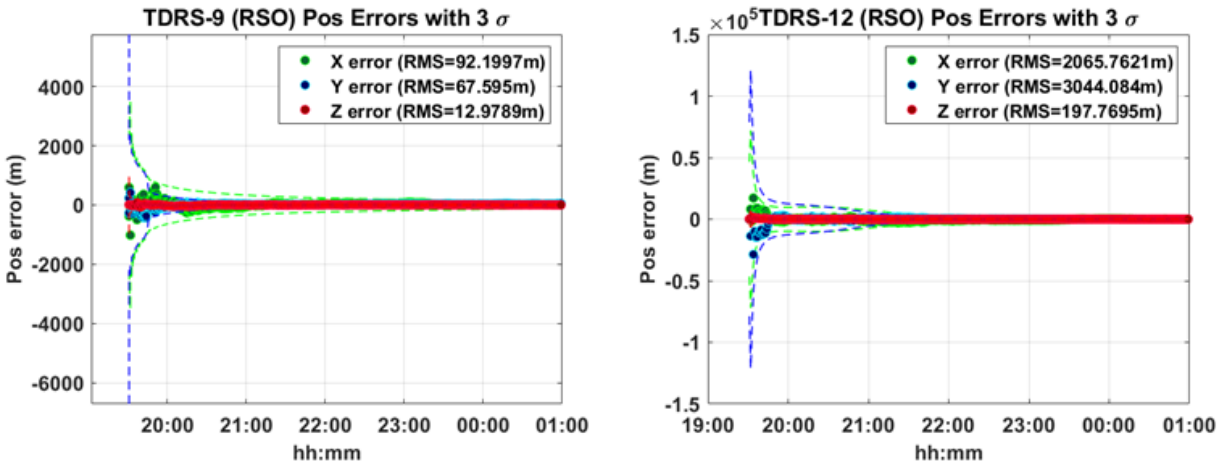

Fig. 5. TDRS-9 (left) and TDRS-12 (right) filter position state errors and 1-sigma uncertainties

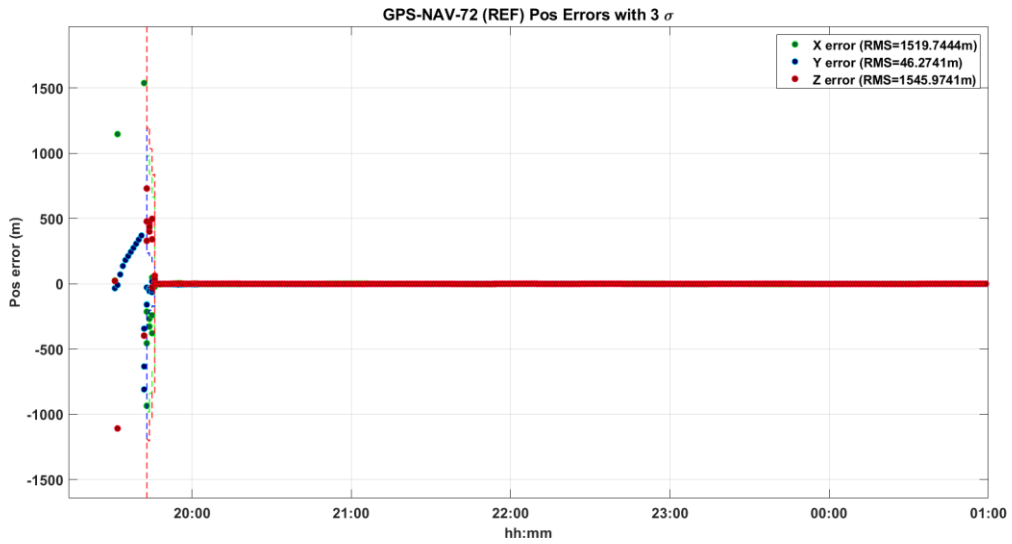

Fig. 6. GPS NAV-72 filter position state errors and 1-sigma uncertainties

Examination of the filter estimates of the timing and range biases shows similar behaviour as summarized in the results provided in Table 5. When the GPS reference state data are included in the USKF processing the bias states converge in minutes, versus hours when no reference state data are used. The sensor timing biases for Southern

Spain for the case where a reference state is used (left) versus when none is used (right) is shown in Fig. 7. Similarly, the range bias for GPS-TRACKER-2 (co-located with the EO tracker in Southern Spain) is shown in Fig. 8 both with (left) and without (right) the reference GPS state included in the USKF.

Table 5. Filter Bias State Estimation for Reference State Sensitivity

		With Refernce State			Without Reference State		
Sensor	**Type**	**Error**	**Sigma**	**Units**	**Error**	**Sigma**	**Units**
SOUTHERN-SPAIN	EO-timing	0.0001	0.0018	seconds	-0.0070	0.0188	seconds
SOUTH-AFRICA	EO-timing	-0.0006	0.0040	seconds	-0.0087	0.0193	seconds
GPS-TRACKER-2	range	-0.310	1.690	meters	1.638	7.624	meters
GPS-TRACKER-3	range	0.139	1.687	meters	0.371	7.884	meters

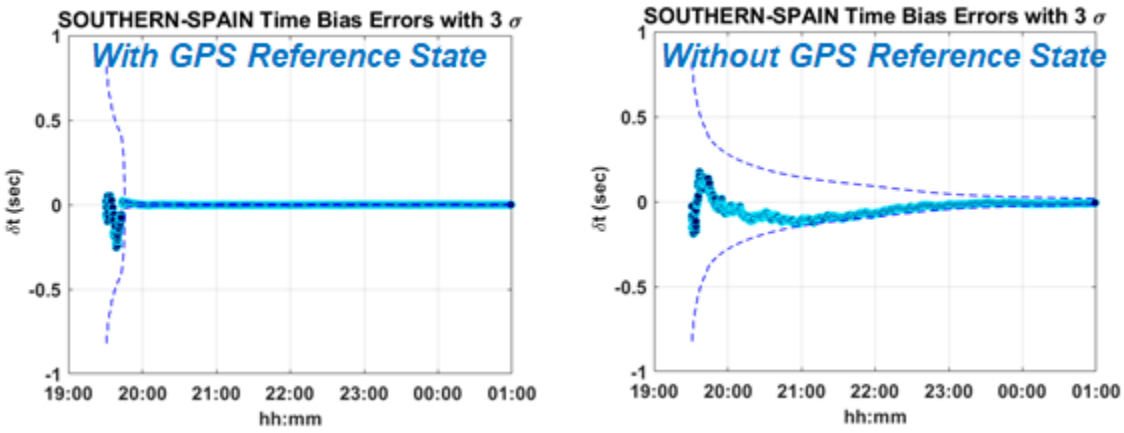

Fig 7. Sensor timing bias estimates with (left) and without (right) reference GPS state

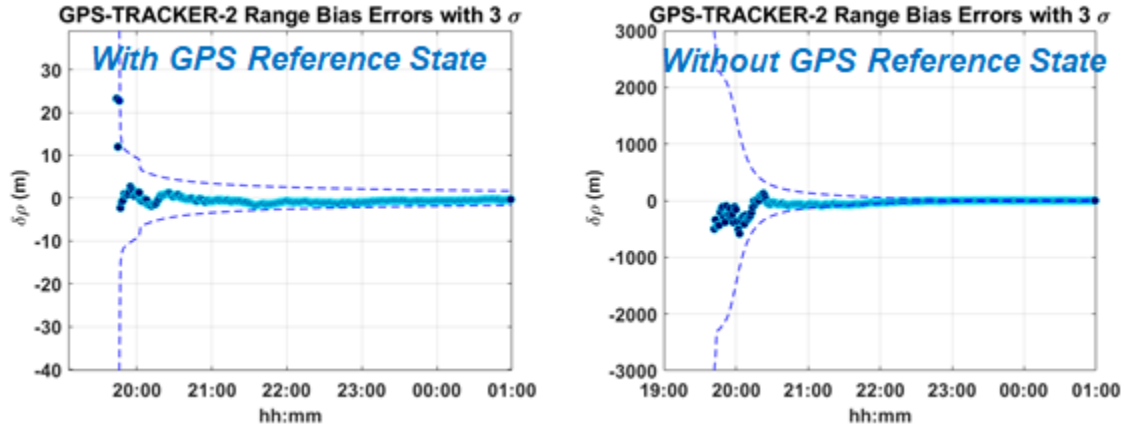

Fig 8. Sensor range bias estimates with (left) and without (right) reference GPS state

Finally, three cases were compared where (1) all timing and range biases were estimated simultaneously, (2) no biases were estimated, and (3) all but one of the range biases were estimated. The purpose was to assess the sensitivity to being able to detect erroneous measurements due to the presence of biases. The pre- and post-fit residuals for the three cases are shown in Fig's 9, 10 ad 11, respectively, with the first and second plots being the pre- and post-fit EO measurement residuals and the third and fourth being the pre- and post-fit range residuals. The residuals in Fig 9 show the obvious normally distributed residuals for a well-behaved filter processing observations containing no biases. Both EO and range residuals for the case where biases are present but not estimated, in Fig 10, show artefacts of the biases in all of the residuals. Finally, in the case where all but the range bias for the South Africa range sensor is estimated, the range residual plots shown in Fig 11 clearly show that the bias is present in the

residuals for that sensor. This means that an automated check of "considered" parameters, e.g. the range bias for the South Africa sensor, could be used as a flag to then enable an estimate of that range bias.

4. CONCLUSIONS AND FUTURE WORK

A near real-time dynamic calibration process was proposed and a prototype implemented which accommodates estimation of sensor related biases when reference data are also available; the biases can also be "considered" prior to estimation. The results indicate the inclusion of an accurate reference state (e.g. use of GPS IGU data to produce an accurate "truth" reference) improved both filter estimation convergence time and accuracy when timing and range measurement biases are estimated. The filter results take much longer to converge when no GPS reference state is included in the filter.

Improvements in the calibration process enable newly vetted sensors to be "trusted" and subsequently used to track non-reference satellites to sufficient accuracy so as to enable them to also be used as references for sensor calibration. The concept demonstrates the value of GPS/GNSS "reference satellites" and access to IGU data which are posted regularly in near real-time. Other sources of reference orbit data provided in NRT that can be leveraged for processing of range used for tracking Low Earth Orbit (LEO) RSOs include high accuracy ephemeris from the International Laser Ranging Service (ILRS). Development is underway to exercise the processes used in this research, and depicted in Fig. 2, to support processing and data conditioning of multiple data types for existing sensor networks.

5. ACKNOWLEDGEMENTS

We would like to Mr. Jason Stauch and Dr. Moriba Jah for their contributions leading up to this work, including their derivations and development of the consider USKF. We would also like to thank the leadership at L3Harris-ADS, in particular Mr. Kirk Carter, Mr. Robert MacMillan and Mr. Tom Kubancik, for supporting both the work and travel to AMOS to present the work. Lastly, we want to thank Mr. Kent Miller and Dr. John Paffett for the originally funded work that served as the basis of this work.

6. REFERENCES

[1] ESA's Annual Space Environment Report, ESA Space Debris Office, GEN-DB-LOG-00271-OPS-SD, Ver. 3.2, 17 July 2019.

[2] Limitations in availability of GEO operational slots: http://scholarlycommons.law.northwestern.edu/cgi/viewcontent.cgi?article=1216&context=njilb

[3] Space Track definition of GEO orbit regime: www.space-track.org

[4] Number of operational satellites in the GEO orbit: http://www.ucsusa.org/nuclear-weapons/space-weapons/satellite-database#.WRHcVojytPY

[5] Kelecy, T., E. Lambert, B. Sunderland, J. Stauch, T. Kubancik, V. Mallik, M. Jah, J. Paffett, N. Sanches-Oritz and Jaime Nomen Torres, "Automated Near Real-time Validation and Exploitation of Optical Sensor Data for Improved Orbital Safety," Proceedings of the 69th International Astronautical Congress, Bremen, Germany, October 2018.

[6] Kelecy, T., E. Lambert, B. Sunderland and J. Stauch, "Automated Near Real-time Validation and Data Integrity Assessment Using an Unscented Schmidt Kalman Filter (USKF)," Proceedings of the Space Flight Mechanics Meeting, Ka'anapali, HI, AAS 19-521, January 13-17, 2019.

[7] Kelecy, T. and M. Jah, "Analysis of Orbit Prediction Sensitivity to Thermal Emissions Acceleration Modeling for High Area-to-mass Ratio (HAMR) Objects," AMOS Technical Conference, Maui, HI, Maui Economic Development Board, 2009.

[8] Wright, J. R., "McReynolds' Filter-Smoother Consistency Test," Internal Analytical Graphics Inc. Internal white paper, May 15, 2009.

[9] Vallado, D., Kelecy, T., and M. Jah, "Data Integrity in Orbital Data Fusion," 63rd International Astronautical Congress. Naples, Italy: International Astronautical Federation, 2012.

[10] Raley, J. et al, "The OrbitOutlook: Autonomous Verification and Validation of Non-Traditional Data for Improved Space Situational Awareness," 17th Advanced Maui Optical and Space Surveillance Technologies (AMOS) Conference. Maui, HI: Maui Economic Development Board, 2016.

[11] Nicolls, M., V. Vittaldev, D. Ceperly, J. Creus-Costam C. Foster, N. Griffith, E. Lu, J. Mason, I. Park, C. Rosner and L. Stepan, "Conjunction Assessment for Commercial Satellite Constellations Using Commercial Radar Data Sources, 2017 AMOS Technical Conference, Wailea, Maui, HI, September 12, 2017.
[12] Tapley, B., B. Schutz and G. Born, Statistical Orbit Determination, Elsevier Academic Press, 2004.
[13] J. Stauch and M. Jah, On the Unscented Schmidt-Kalman Filter Algorithm. Journal of Guidance, Control, and Dynamics 38(1): 117-123, 2014.
[14] Flohrer, C. (2008), "Mutual validation of satellite-geodetic techniques and its impact on GNSS orbit modeling," Zürich, Switzerland: Schweizerische Geodätische Kommission, Institut für Geodäsie und Photogrammetrie, Eidg. Technische Hochschule Zürich.

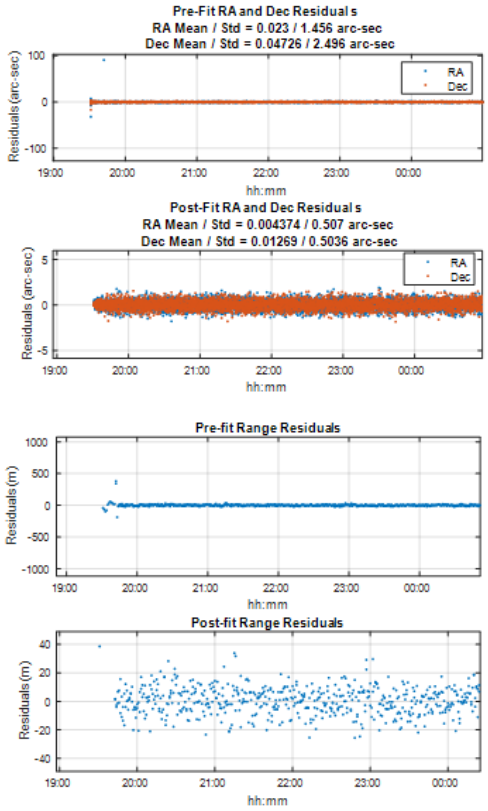

Fig 9. EO and range residuals with all timing and range biases estimated

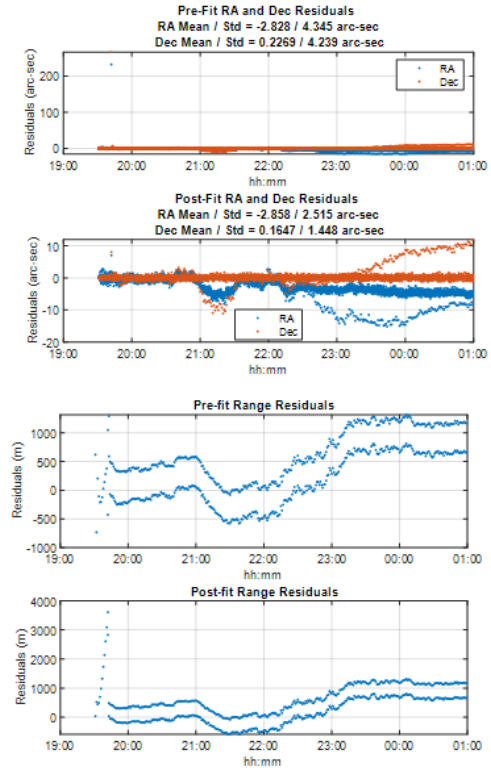

Fig 10. EO and range residuals with all no biases estimated

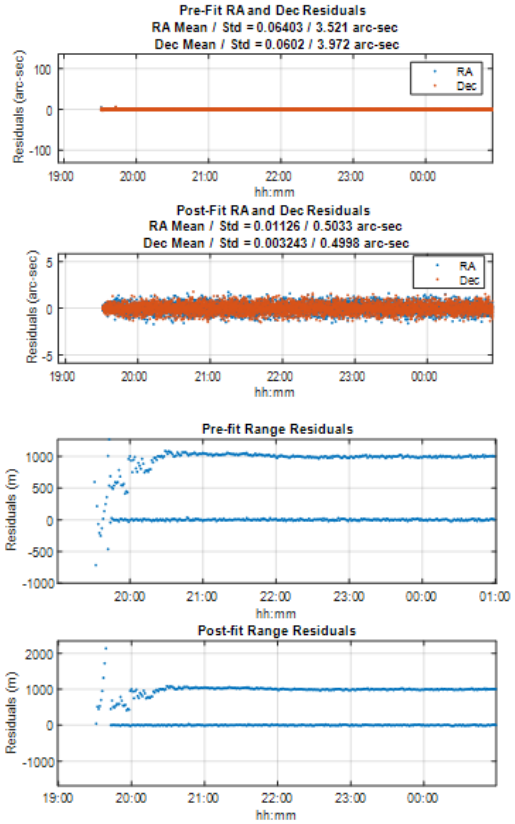

Fig 11. EO and range residuals with all but one sensor range biases estimated